# Modulation Response of Monolithically Integrated External Optical Injection-Locking Semiconductor Ring Laser Based on PPR Effect

Ben Zhang [ID], Ruiying Zhang [ID], Shujie Xu, Chanchan Luo, and Bocang Qiu

*Abstract*—The modulation response of monolithically integrated external optical injection-locking (EOIL) semiconductor ring lasers based on photon-photon resonance effect was systematically analyzed. The simulation results show that the modulation response of the EOIL laser is strongly dependent on the internal loss of the ring laser. Assuming that the waveguide was loss-free, the modulation bandwidth of as high as 67.5 GHz was predicted. However, due to the excessive loss associated with the bending waveguide of the circular-shaped ring laser, the modulation performance of such EOIL laser has no any advantage over its free-running counterpart. Instead, use of rectangular-shaped ring laser as the slave laser is proposed to circumvent the issue associated with the excessive waveguide loss, since the internal loss, in this case, is only dependent on the reflectivity of the total reflection mirrors. Simulation shows the modulation bandwidth of at least 38 GHz is achievable in such EOIL laser, provided the reflectivity of the total reflection mirrors is greater than 96%. It is believed that this theoretical study will facilitate the future experimental demonstration of the monolithically integrated EOIL lasers.

*Index Terms*—Direct modulation lasers, external optical injection-locking, monolithically integrated, photon-photon resonance, ring lasers.

## I. INTRODUCTION

**D**UE to the rapidly growing demand for greater data transmission capacity in optical communication networks,

Ben Zhang is with the School of Nano-Tech and Nano-Bionics, University of Science and Technology of China, Hefei 230026, China, with the Nano-Devices and Materials Division, Suzhou Institute of Nano-Tech and Nano-Bionics, Chinese Academy of Science, Suzhou 215123, China, and also with the Nano Science and Technology Institute, University of Science and Technology of China, Suzhou 215123, China (e-mail: bzhang2020@sinano.ac.cn).

Ruiying Zhang and Chanchan Luo are with the School of Nano-Tech and Nano-Bionics, University of Science and Technology of China, Hefei 230026, China, the Nano-Devices and Materials Division, Suzhou Institute of Nano-Tech and Nano-Bionics, Chinese Academy of Science, Suzhou 215123, China, with Key Laboratory of Nanodevices and Applications, Suzhou Institute of Nano-Tech and Nano-Bionics, Chinese Academy of Science, Suzhou 215123, China, and also with Suzhou Institute of Nano-Tech and Nano-Bionics, Chinese Academy of Science, Nanchang (SINANONC) 330200, China (e-mail: ryzhang2008@sinano.ac.cn; ccluo2018@sinano.ac.cn).

Shujie Xu and Bocang Qiu are with the Institute of Atomic and Molecular Science, Shaanxi University of Science and Technology, Xi'an 710021, China, and also with the Nano-Devices and Materials Division, Suzhou Institute of Nano-Tech and Nano-Bionics, Chinese Academy of Science, Suzhou 215123, China (e-mail: sjxu2020@sinano.ac.cn; 4407@sust.edu.cn).

there is an urgent need for a significant increase in the transmission rate of light sources [1], [2]. Directly modulated lasers (DMLs), which refer to semiconductor lasers with a directly loaded modulation signal, become more attractive, because of their advantages in cost, power consumption, and chip size. A modulation bandwidth is the most important parameter for DML employed in such domain as it determines the transmission rate [3].

At present, due to the intrinsic limitation induced by RC constants, it becomes very difficult to further improve the modulation bandwidth of conventional DMLs that is based on the carrier-photon resonance (CPR) [4], [5]. External optical injection-locking (EOIL) is one of the most promising schemes that utilize the photon-photon resonance (PPR) to realize optical frequency synchronization, and to achieve the modulation bandwidth beyond that ordinary DMLs can reach [6], [7], indeed the modulation bandwidth as high as 72 GHz has been demonstrated [8]. However, such EOIL lasers were realized only by discrete fiber system, as an isolator has to be required to ensure the unidirectional injection of the master laser to the slave laser [9].

Meanwhile, attention has also been paid to the phenomenon that a ring laser can be unidirectionally injection-locked [10], M. I. Memon *et al.* built an EOIL experimental system with a tunable laser, a semiconductor ring laser (SRL), and other discrete components, and demonstrated the modulation bandwidth of 40 GHz [11]. The experiment also shows that an isolator-free EOIL laser can be realized by using ring laser as a slave laser. Thereafter, L. Chrostowski *et al.* further proposed a monolithically integrated optically injection-locked SRL and simulated its modulation performance, where the modulation bandwidth of over 40 GHz was envisaged under a high injection ratio [12]. Then, G. A. Smolyakov *et al.* proposed an EOIL prototype of monolithically integrated DBR laser strong injection-locking whistle-geometry semiconductor ring laser [13], [14], and predicted the relaxation resonance frequency of 160 GHz. This is perhaps the highest relaxation resonance frequency for a semiconductor laser to be able to achieve. Theoretical studies have shown that monolithically integrated EOIL lasers are able to produce truly excellent modulation bandwidth, which is far beyond that determined by the CPR. In addition, compared with the traditional DML, higher output power will be potentially achieved in such EOIL lasers, as their output power is mainly determined by the master laser, but the modulation bandwidth is mainly determined by
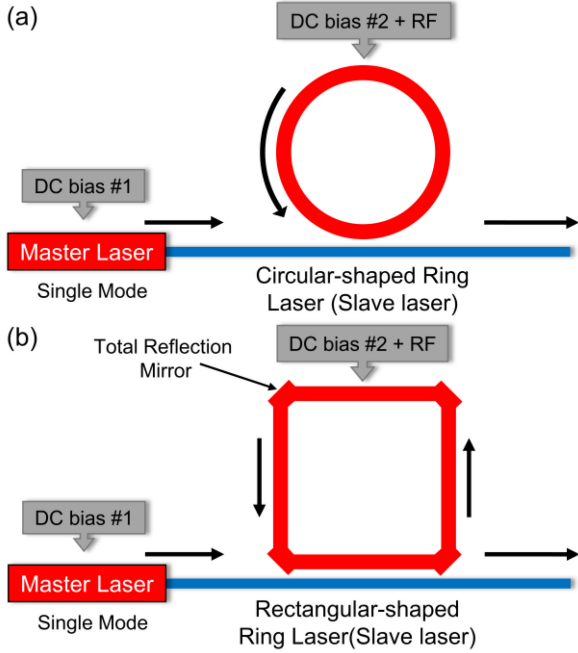
Fig. 1. Monolithically integrated externally optical injection-locking laser with a different type slave laser. (a) A circular-shaped ring laser. (b) A rectangular-shaped ring laser.

the slave laser. However, a truly monolithic EOIL laser has not been realized yet. Only simulations were performed as above mentioned based on the assumption that the ring laser was loss-free. Obviously, this is not true in an actual semiconductor ring laser.

In this paper, modulation response of monolithically integrated EOIL lasers was theoretically studied, and internal loss was introduced to our slave ring laser to understand the impact of the loss on the modulation performance. Our simulation also shows that once the bending loss is accounted, monolithically integrated EOIL lasers with a circular-shaped ring structure no longer produce stronger modulation performance than their free-running counterparts. As an alternative, one can choose a rectangular-shaped ring laser as the slave laser. In this case, the modulation bandwidth of such EOIL lasers is mainly dependent on the reflectivity of the total reflection mirrors (TRMs). The modulation bandwidth of over 38 GHz is predicted once the reflectivity of the TRMs is more than 96%. It is believed that this study is beneficial to the understanding of modulation behaviors of EOIL lasers, and provides a theoretical basis for the future experiment demonstration of monolithic integrated EOIL semiconductor lasers.

## II. MODELS AND SIMULATIONS

A monolithically integrated EOIL laser is schematically shown in Fig.1, where a circular-shaped ring laser (as shown in Fig. 1(a)) or a rectangular-shaped ring laser (as shown in Fig. 1(b)) acting as a slave laser, is injection-locked by a single-mode master laser. Due to the inherent travelling wave property

of ring resonators, this type of injection-locking laser is essentially a kind of highly unidirectional transmission system, where counterclockwise (CCW) mode will be locked and clockwise (CW) mode will be greatly suppressed. Therefore, the feedback of CW mode to the master laser is ignored. In addition, the master laser and the slave laser are coupled through a passive bus waveguide and the RF signal is loaded on the ring laser.

To investigate the characteristics of this EOIL laser, we first begin with establishing a single-mode master laser model based on the rate equations, which are expressed according to the photon numbers $S_m$ and the phase $\theta_m$, assuming that the carrier density and the photon density are uniform in the laser cavity

$$\frac{dS_m}{dt} = \left[ G_{0m} \left( N_m - N_{0m} \right) - \frac{1}{\tau_{pm}} \right] S_m + R_{spm} \quad (1)$$

$$\frac{d\theta_m}{dt} = \frac{\alpha}{2} \left[ G_{0m} \left( N_m - N_{0m} \right) - \frac{1}{\tau_{pm}} \right] \quad (2)$$

$$\frac{dN_m}{dt} = \eta_i \frac{I_m}{q} - \frac{N_m}{\tau_c} - G_{0m} \left( N_m - N_{0m} \right) S_m \quad (3)$$

In (1)–(3), $G_{0m}$ and $R_{spm}$ are differential mode gain and spontaneous emission rate of the master laser, respectively, given by the following formula

$$G_{0m} = \frac{\Gamma * a * \nu_g}{V_m}, \; R_{spm} = n_{sp} * G_m \quad (4)$$

Where $\alpha$ is the linewidth enhancement factor, $\Gamma$ is the optical confinement factor, $a$ is the differential gain, $v_g$ is the group velocity, $\eta_i$ is the internal quantum efficiency, q is the electronic charge, $\tau_c$ is the carrier lifetime, $N_m$, $N_{0m}$, $\tau_{pm}$ and $V_m$ are the carrier number, the transparent carrier number, the photon lifetime and the active volume of the master laser, respectively, $n_{sp} = 2.6$, is the Fermi inversion factor [15].

The rate equations for a ring laser are expressed according to the photon numbers $S_{cw}$, $S_{ccw}$ and the phase $\theta_{cw}$, $\theta_{ccw}$ of CW mode and CCW mode

$$\frac{dN_r}{dt} = \eta_i \frac{I_r}{q} - \frac{N_r}{\tau_c} - G_{cw} S_{cw} - G_{ccw} S_{ccw} \quad (5)$$

$$\frac{dS_{ccw}}{dt} = \left[ G_{ccw} - \frac{1}{\tau_{pr}} \right] S_{ccw} + R_{spccw}$$
$$+ 2\kappa_c \sqrt{S_m S_{ccw}} \cos \left( \Delta \theta \right) \quad (6)$$

$$\frac{d\theta_{ccw}}{dt} = \frac{\alpha}{2} \left[ G_{ccw} - \frac{1}{\tau_{pr}} \right] - \Delta \omega - \kappa_c \sqrt{\frac{S_m}{S_{ccw}}} \sin \left( \Delta \theta \right) \quad (7)$$

$$\frac{dS_{cw}}{dt} = [G_{cw} - \frac{1}{\tau_{pr}}] S_{cw} + R_{spcw} \quad (8)$$

$$\frac{d\theta_{cw}}{dt} = \frac{\alpha}{2} \left[ G_{cw} - \frac{1}{\tau_{pr}} \right] - \Delta \omega \quad (9)$$

$$G_{cw} = \frac{G_{0r} \left( N_r - N_{0r} \right)}{1 + \varepsilon_s S_{cw}/V_r + \varepsilon_c S_{ccw}/V_r} \quad (10)$$

$$G_{ccw} = \frac{G_{0r} \left( N_r - N_{0r} \right)}{1 + \varepsilon_s S_{ccw}/V_r + \varepsilon_c S_{cw}/V_r} \quad (11)$$

In (5)–(11), $G_{0r}$ is the differential mode gain of ring laser, $R_{spcw}$, $R_{spccw}$ are the spontaneous emission rate of CW mode

and CCW mode, respectively, given by the following formula

$$G_{0r} = \frac{\Gamma * a * \nu_g}{V_r}, \ R_{spcw} = n_{sp} * G_{cw}, \ R_{spccw} = n_{sp} * G_{ccw} \tag{12}$$

Where $\Delta\omega = (\omega_0 - \omega_{th})$ is the angular frequency detuning, which is the difference of the lasing frequency between the master laser and the slave laser, $\Delta\theta = (\theta_{ccw} - \theta_m)$ is the phase detuning between CCW mode of the ring laser and the master laser. $N_r$, $N_{0r}$, $\tau_{pr}$ and $V_r$ are the carrier number, the transparent carrier number, the photon lifetime and the active volume of the ring laser, respectively, $\kappa_c$ is the injection coupling rate, $\varepsilon_s$ and $\varepsilon_c$ are the gain self-saturation coefficients and the gain cross-saturation coefficients, respectively, which adopt the typical values [16]. It should be noted that the linear coupling between CW mode and CCW mode is ignored, due to the linear coupling is a perturbation term when the ring laser is biased at high current [17].

In (7), $S_m / S_{ccw} = R_{int}$. We define $R_{int}$ as an internal injection ratio which means the ratio of the power injected into the cavity to the power of free-running slave laser. $R_{ext}$, referred to as the external injection ratio, is the ratio of the injection power incident onto the slave laser to the output power of the free-running slave laser. By referring to the relationship deduced by Lau *et al.* [18], we can obtain the ratio of $R_{int}$ to $R_{ext}$ to calculate the injection coupling rate $k_c$

$$k_c = \frac{1}{\tau_{rt}} \sqrt{\frac{R_{int}}{R_{ext}}} = \frac{c}{nL} \frac{1 - t^2}{t} \tag{13}$$

Finally, to simulate the impact of internal loss on the modulation bandwidth of EOIL lasers, we introduce the internal loss $\alpha_{i1}$ and $\alpha_{i2}$ into the photon lifetime $\tau_{pm}$ and $\tau_{pr}$

$$\tau_{pm} = \frac{1}{\frac{c}{n_{eff}} \left( -\frac{\ln\sqrt{R}}{L_m} + \alpha_{i1} \right)} \tag{14}$$

$$\tau_{pr} = \frac{1}{\frac{c}{n_{eff}} \left( -\frac{\ln t}{L_r/2} + \alpha_{i2} \right)} \tag{15}$$

$$\alpha_{i1} = \alpha_{int} + \alpha_{sc} \tag{16}$$

$$\alpha_{i2} = \alpha_{int} + \alpha_{sc} + \alpha_{bend}$$
$$\text{or } \alpha_{i2} = \alpha_{int} + \alpha_{sc} + \frac{4}{L_r} ln\left(\frac{1}{r_t}\right) \tag{17}$$

Where $r_t$ is the reflection coefficient of the TRMs, $\alpha_{int}$, $\alpha_{sc}$ and $\alpha_{bend}$ are the intrinsic waveguide loss, the scattering loss and the bending loss, respectively.

Table I lists the parameters used in our simulation, a compressive-strained InGaAs/InGaAsP/InP 4 QWs (total thickness is 45nm) epitaxial structure with a lasing wavelength of 1550 nm is used as the material structure. The width of ridge waveguide and the length of the master laser's active region are set to 1.5 $\mu$m and 300 $\mu$m, respectively. The ring laser has the identical epitaxy structure and as well as ridge waveguide structure to that for the master laser. To avoid excessively long list in Table I, only the parameters of the ring laser with cavity length of 62.83 $\mu$m and internal loss of 6.2 cm$^{-1}$ are listed. To make it easier to distinguish, the cavity length of the ring laser is rounded up or down in the next section.

TABLE I
INJECTION-LOCKED LASER PARAMETERS

| Parameters | Symbol | Value | Units |
|---|---|---|---|
| **Material Parameters** | | | |
| Linewidth enhancement factor | $\alpha$ | 4 | |
| Carrier lifetime | $\tau_c$ | 0.4 | ns |
| Differential gain | $a$ | $1\times10^{-15}$ | cm$^2$ |
| Optical confinement factor | $\Gamma$ | 0.09 | |
| Group refractive index | $\alpha_g$ | 3.42 | |
| Group velocity | $v_g$ | $8.76\times10^9$ | cm/s |
| Internal quantum efficiency | $\eta_i$ | 0.75 | |
| Transparency carrier density | $N_0 / V$ | $0.485\times10^{18}$ | cm$^{-3}$ |
| **Master Laser** | | | |
| Effective refractive index | $n_{eff}$ | 3.2 | |
| reflection coefficients | $R = r_1 \times r_2$ | $1 \times 0.85$ | |
| Cavity length | $L_m$ | 300 | $\mu$m |
| Ridge waveguide width | $d_m$ | 1.5 | $\mu$m |
| Active volume | $V_m$ | $2.025\times10^{-11}$ | cm$^3$ |
| Photon lifetime | $\tau_{pm}$ | 12.2484 | ps |
| **Ring Laser** | | | |
| Injection coupling rate | $k_c$ | $2.4262\times10^{11}$ | s$^{-1}$ |
| Effective refractive index | $n_{eff}$ | 3.2 | |
| coupling coefficient | $t, k$ | 0.922, 0.387 | |
| Ridge waveguide width | $d_r$ | 1.5 | $\mu$m |
| Cavity length | $L_r$ | 62.83 | $\mu$m |
| Active volume | $V_m$ | $4.2410\times10^{-12}$ | cm$^3$ |
| Photon lifetime | $\tau_{pm}$ | 3.3281 | ps |
| Self-nonlinear gain saturation | $\varepsilon_s$ | $2.7\times10^{-18}$ | cm$^3$ |
| Cross-nonlinear gain saturation | $\varepsilon_c$ | $5.4\times10^{-18}$ | cm$^3$ |

Based on the above model and parameters listed in Table I, the steady-state characteristics of the EOIL laser is simulated by solving (1)–(3) and (5)–(9) using the fourth-order Runge-Kutta method, then the small signal modulation response of injection locked lasers is calculated and finally normalized to DC free-running response, assuming that the ring laser injection current is set to $I_r = I_{r0} + I_{r1} \exp (j\omega t)$ and carrier lifetime $\tau_c$ is fixed. In order to provide a reference for EOIL lasers, the modulation response of the free-running ring lasers is also simulated by solving (5)–(9) with $S_m = 0$.

## III. RESULTS AND DISCUSSION

Fig. 2 illustrates the steady-state characteristics of EOIL lasers with different ring cavity lengths within their injection-locking range. As shown in Fig. 2(a) and 2(b), both the carrier density and the photon density in the ring cavity exhibit asymmetric distributions with their frequency detuning, which corresponds to the asymmetric injection-locking range induced by the linewidth enhancement factor. Meanwhile, the distributions become narrower with the increased ring cavity length, which is also related to the corresponding injection-locking range and their free-spectrum-range. Further referring to Figs. 2(a), (b) and (c), one can conclude that the EOIL lasers are always in a locking state in their whole frequency detuning range, the phase detuning gradually decreases from $\pi/2$ to $-\pi/2$ with their frequency detuning. Moreover, one can see that the zero phase detuning points correspond to the minimum carrier density and
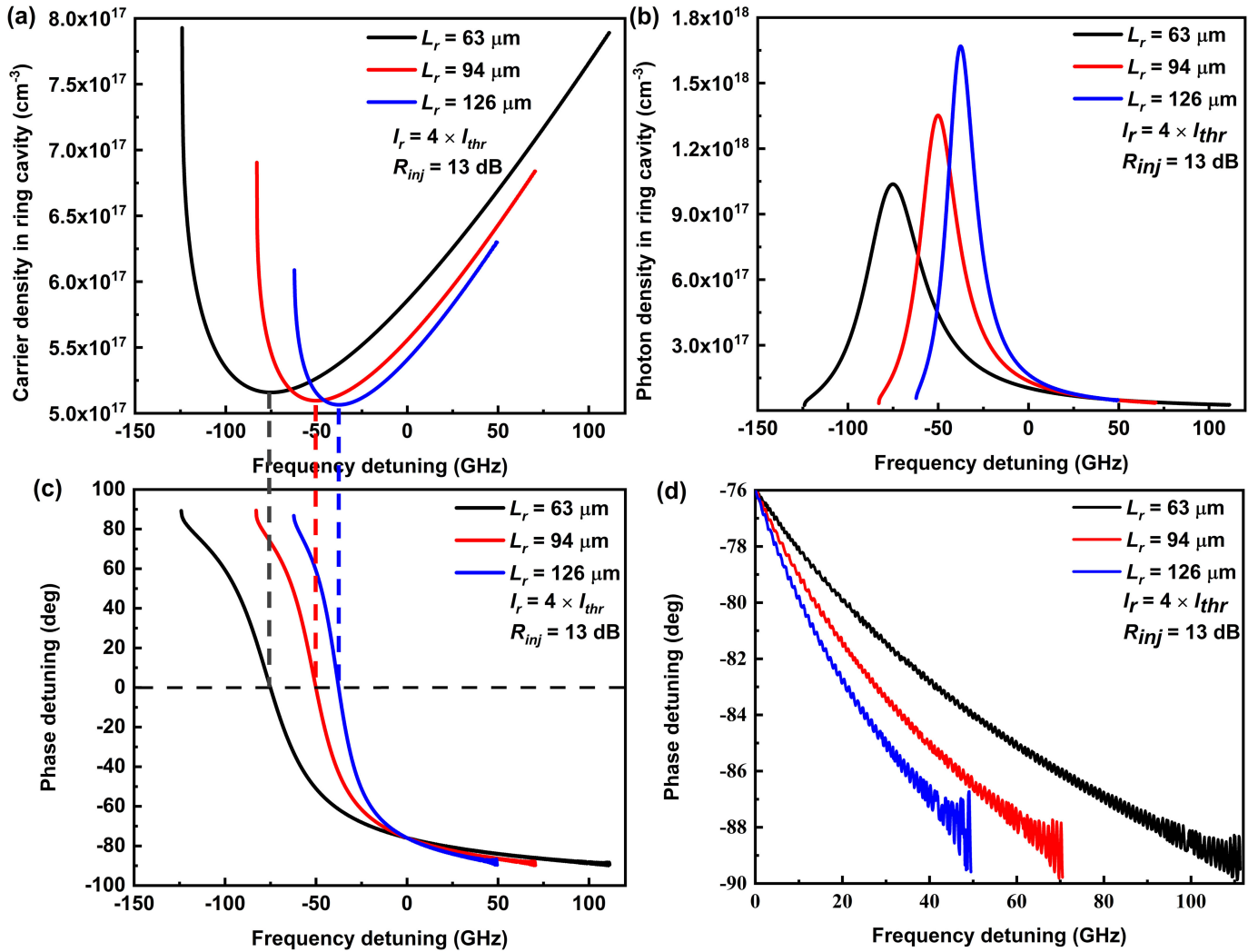
Fig. 2. Steady-state characteristics of the EOIL laser. (a) Carrier density versus frequency detuning. (b) Photon density versus frequency detuning. (c) Phase detuning versus frequency detuning. (d) Phase detuning versus positive frequency detuning.

the maximum photon density, which means the EOIL laser has the highest locking efficiency when its phase matching happens between the master laser and the CCW mode of the slave laser.

On the other hand, when the phase detuning is far away from zero, both the increase in the carrier density and the decrease in the photon density are observed, which is due to the destructive interference between the master lasing mode and the CCW mode in the slave laser [19]. It is worth noting that the phase-matching point is actually dependent on the cavity length. The longer the cavity, the more the phase-matching point shifts to the right, and this can be explained by the fact that the injection coupling rate $k_c$ is inversely proportional to the ring cavity length. In addition, from Fig. 2(a)–(c) one can see that a large phase detuning, a higher carrier density and especially a lower photon density occur when the frequency detuning is zero, which indicates that self-injection locking is not an optimized injection-locking state in this situation. As a result, external-injection locking, due to its frequency detuning can be adjusted, is a more adequate approach to achieving better injection-locking performance. Fig. 2(d)

shows the phase detuning with the positive frequency detuning. Obviously, the phase detuning becomes increasingly unstable with the increase in the detuning, which indicates that the injection-locking is unstable and even out of locking. Therefore, such EOIL laser cannot operate in these conditions.

Fig. 3 shows the small signal modulation response curves of EOIL lasers with zero-loss ring lasers with different bias currents, injection ratios and cavity lengths. The red arrow indicates the maximum modulation bandwidth under injection-locking, which is much larger than that in the free-running mode indicated by the black arrow. This shows that EOIL laser with PPR effect can indeed expand the modulation bandwidth of traditional DML. Comparing Fig. 3(a) with 3(b), one can see that the modulation response curve becomes flatter and higher modulation bandwidth of 42.9 GHz is achievable, when the bias current is increased from $4 \times I_{thr}$ to $6 \times I_{thr}$. This is due to the improvement of the photon density in the cavity, which in turn leads to improved low-frequency drop off effect [20] at the positive frequency detuning. Comparing Fig. 3(b) with 3(c),
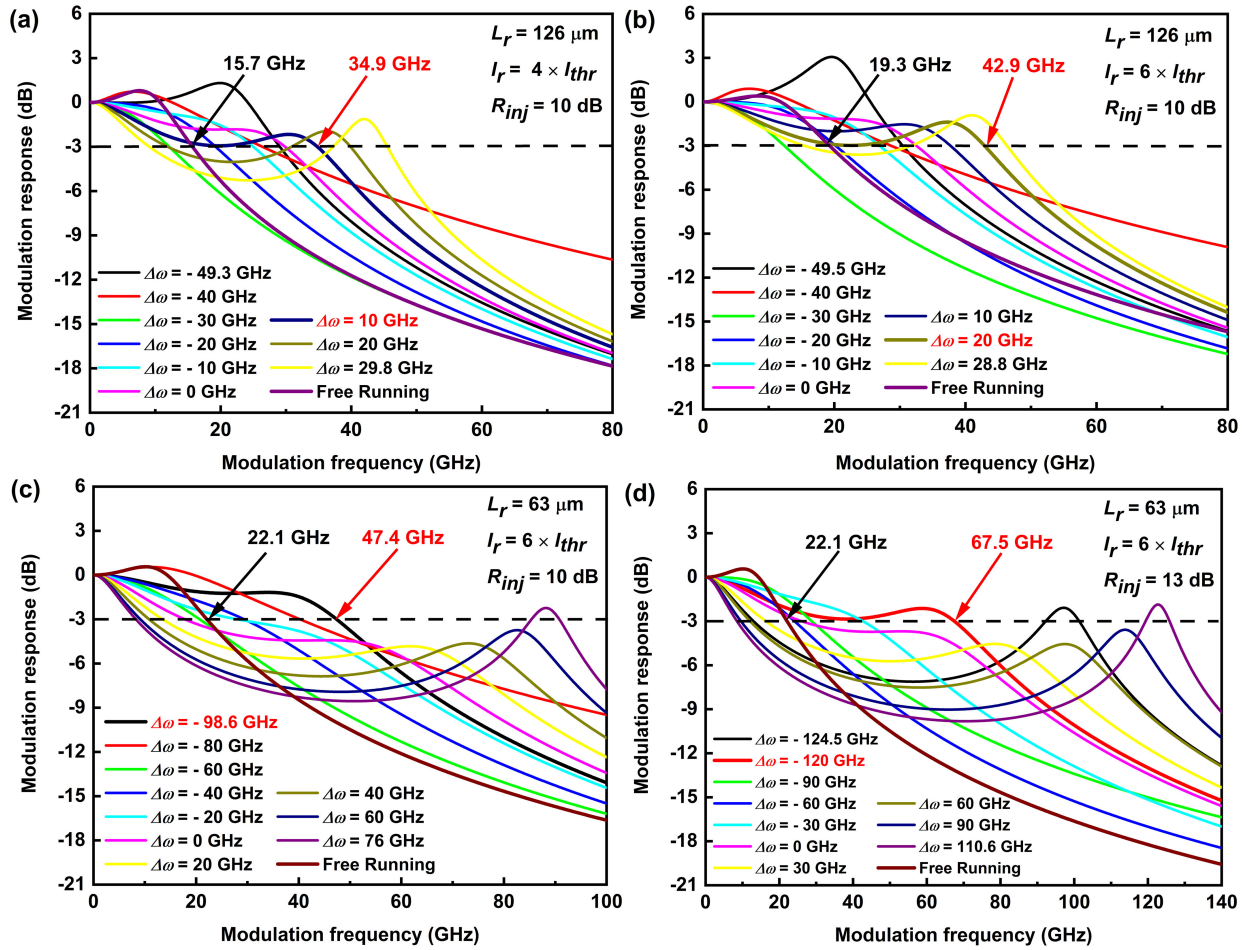
Fig. 3. The small signal modulation response of EOIL laser (a) $I_r = 4 \times I_{thr}$, $R_{inj} = 10$ dB, $L_r = 126$ $\mu$m. (b) $I_r = 6 \times I_{thr}$, $R_{inj} = 10$ dB, $L_r = 126$ $\mu$m. (c) $I_r = 6 \times I_{thr}$, $R_{inj} = 10$ dB, $L_r = 63$ $\mu$m. (d) $I_r = 6 \times I_{thr}$, $R_{inj} = 13$ dB, $L_r = 63$ $\mu$m.

one can see that there is only a very limited improvement in the modulation bandwidth, even though the cavity length is reduced by half and the injection coupling rate is doubled. The reason is that although the resonance frequency increases significantly, there will also be a more obvious low-frequency drop off effect. The effect of the injection ratio can be clearly seen by comparing Fig. 3(c) with (d). When the injection ratio is increased from 10 dB to 13 dB, the resonance frequency increases to 120 GHz from about 86 GHz, while the maximum modulation also improves bandwidth from 47.4 GHz to 67.5 GHz, which indicates that such improvement increase of the modulation bandwidth is due to the increase in the resonance frequency induced by the injection ratio.

The above results and discussion are based on the assumption that the EOIL laser is lossless. To obtain a real picture that happened in the real world for EOIL semiconductor lasers, the impact of cavity loss in the ring laser on the dynamic performance of the EOIL lasers must be addressed. Here, we set the cavity length of the ring laser to be $L_r = 63$ $\mu$m, injection ratio to be $R_{inj} = 13$ dB, and bias current to be $I_r = 6 \times I_{thr}$, respectively. In addition, assuming that the internal loss of master laser is fixed to 6.2 cm$^{-1}$, which accounts for the loss related to the free carrier absorptions occurred both in the cladding layers and in

the active region, but the internal loss of ring lasers is varied from 6.2 cm$^{-1}$ to 30.2 cm$^{-1}$, here the excessive loss accounts for that arisen from the bending waveguide loss, or from the imperfect reflection of the TRMs.

Fig. 4(a) and (b) shows the modulation response of the EOIL laser when the internal loss of ring laser is 6.2 cm$^{-1}$ and 14.2 cm$^{-1}$, respectively. Compared with Fig. 3(d) in which the ring laser is loss-free, even though a similar modulation response has been observed in these EOIL lasers, the overall reduced modulation amplitude, the aggravated low-frequency drop off, the increased modulation bandwidth at free-running state, and the decreased modulation bandwidth at injection-locking state, are observed, also. These phenomena can be contributed to the reduced photon lifetime induced by the internal loss. Fig. 4(c) shows the modulation response of the EOIL lasers with the lossy ring lasers at free-running state and the maximum modulation bandwidth state, when the internal loss of ring laser varies from 14.2 cm$^{-1}$ to 38.2 cm$^{-1}$. It is obvious that the modulation bandwidth of free-running ring lasers increases slightly with the internal loss, but the modulation bandwidth of EOIL lasers reduces quickly with the internal loss. This means that the difference between the modulation bandwidth for the EOIL laser and the free-running ring laser decreases sharply with
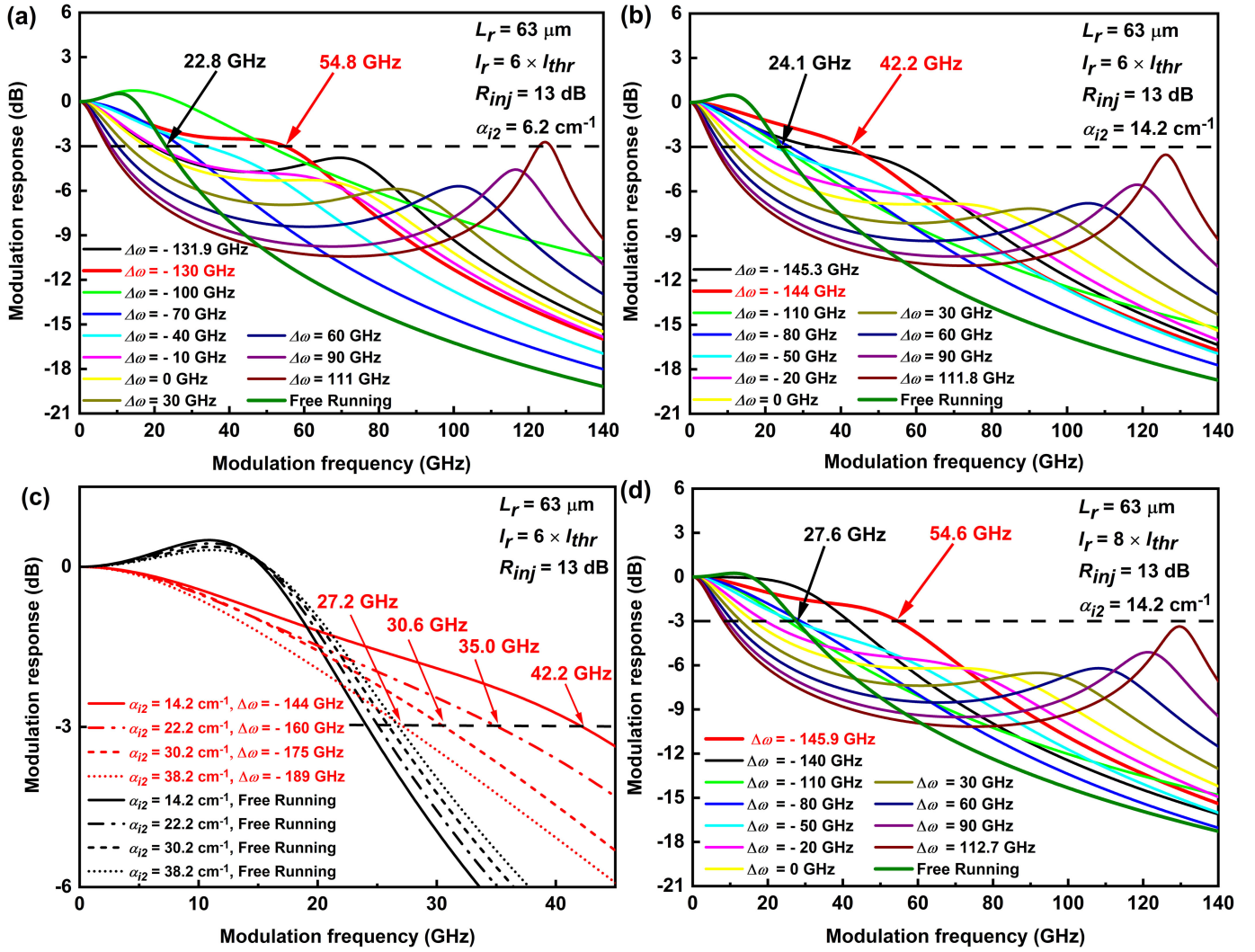
Fig. 4. The modulation response of EOIL laser when $L_r = 63$ $\mu$m, $R_{inj} = 13$ dB. (a) $I_r = 6 \times I_{thr}$, $\alpha_{i2} = 6.2$ cm$^{-1}$. (b) $I_r = 6 \times I_{thr}$, $\alpha_{i2} = 14.2$ cm$^{-1}$. (c) $I_r = 6 \times I_{thr}$, $\alpha_{i2} = 14.2$ cm$^{-1}$, 22.2 cm$^{-1}$, 30.2 cm$^{-1}$, 38.2 cm$^{-1}$. (d) $I_r = 8 \times I_{thr}$, $\alpha_{i2} = 14.2$ cm$^{-1}$.

the internal loss. When the internal loss is 38.2 cm$^{-1}$, the modulation bandwidth in free-running state is basically the same as that in injection-locking state. These results indicate that the advantages of PPR over CPR is dependent on the internal loss. Therefore, a ring laser with low internal loss is very crucial for achieving high modulation bandwidth.

Comparing Fig. 4(b) with 4(d), one can see that when the bias current is increased from $6 \times I_{thr}$ to $8 \times I_{thr}$, the modulation bandwidth of the free-running ring laser has a slight increase from 24.1 GHz to 27.6 GHz, the modulation bandwidth of the EOIL laser increases from 42.2 GHz to 54.6 GHz due to the weakening of the low-frequency drop off effect in the modulation response curve. Such results indicate that the internal loss exacerbates the modulation response and further reduces the modulation bandwidth of the EOIL laser, other methods can be further adopted to improve their performance according to its low-frequency drop off effect, such as using cascaded ring lasers [14], modulating the master laser [21] and using Q-modulation instead of current modulation [22].

Fig. 5 summarizes the dependence of the maximum modulation bandwidth on the internal loss of the ring lasers as well as the ring cavity length, the modulation bandwidths of zero-loss EOIL lasers are also listed for comparison. Apparently, the maximum modulation bandwidth of such EOIL lasers decreases with the increase of both the internal loss and the cavity length. Moreover, when the internal loss is low, EOIL lasers perform better than their free-running counterparts, however, the performance difference will diminish, after the certain point, and the point is hereafter referred to as the cut-off internal loss (COIL). From the plots in Fig. 5, one can see that even though the COIL of the 63 $\mu$m, 94 $\mu$m and 126 $\mu$m long ring laser is about 38.2 cm$^{-1}$, 30.2 cm$^{-1}$ and 22.2 cm$^{-1}$, respectively, the modulation bandwidth at COIL point decreases slowly and basically keeps at about 25 GHz. Such a phenomenon means that the maximum available modulation bandwidth of EOIL laser is mainly determined by the dependence of the loss on the cavity length. As a result, if the loss is strongly dependent on the cavity length, a longer ring laser should be better to achieve the modulation bandwidth operate at
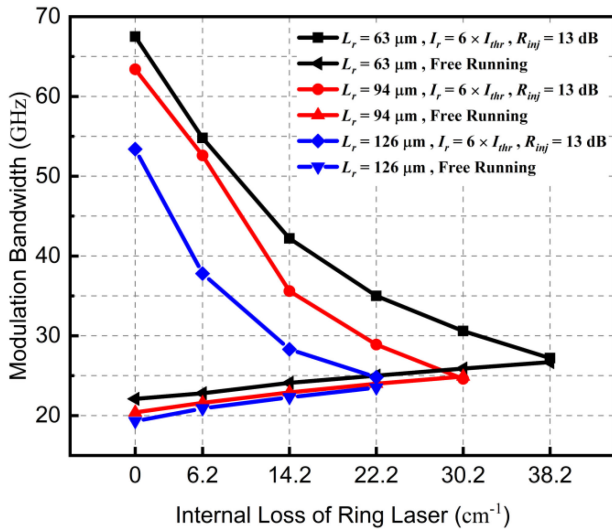
Fig. 5. The modulation bandwidth of EOIL laser versus internal loss of ring laser with different ring cavity length.
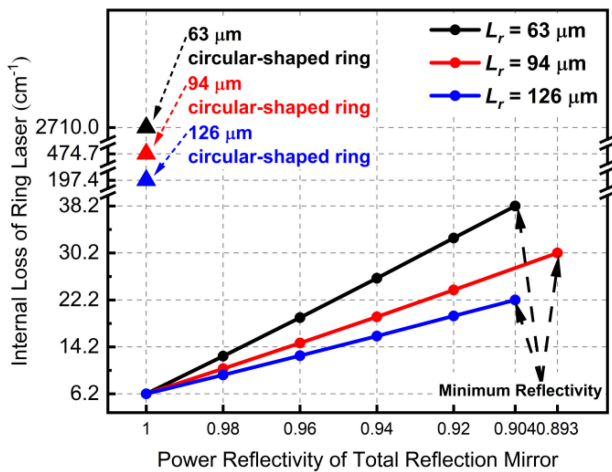


Fig. 6. The internal loss of the rectangular-shaped ring lasers verses the power reflectivity of TRMs. The triangular points show the internal loss of the circular-shaped ring lasers.

the COIL point. Otherwise, a shorter ring laser is beneficial to achieve a higher modulation bandwidth.

Fig. 6 plots the relationship between internal loss of rectangular-shape ring lasers and the reflectivity of the TRMs, the bending losses for circular-shaped waveguide lasers are also marked in the plot. The actual optical losses for a ring waveguide laser come from several sources, including the loss associated with the free carrier absorption (FCA) in the active region as well as in the cladding layers, the bending loss in case the waveguide is circular-shaped, or the loss related to the reflectivity of the TRMs in the rectangular-shaped waveguide configuration. In our design, the waveguide loss related to the FCA is around 6.2 cm$^{-1}$. We performed the calculation of the bending loss for shallow-etched ring waveguide, and it was found that the bending loss is highly sensitive to the waveguide curvature. For example, when the circumference (or the total cavity length)

of the ring waveguide is 63 $\mu$m, the bending loss is 2710.0 cm$^{-1}$, which will be reduced to 197.4 cm$^{-1}$, if circumference is increased to 126 $\mu$m. From Figs. 5 and 6, it is certain that EOILs with circular-shaped waveguide are no longer a choice for applications which require the modulation bandwidth performance over 25 GHz, due to the excessive loss associated with the bending waveguide are far higher than their COIL. Instead, rectangular-shaped configuration can be considered, since the loss associated with it mainly depends on the reflectivity of the TRMs, as is shown in Fig. 6. In fact, when the power reflectivity of TRMs is 90.4%, the internal losses for 63 $\mu$m and 126 $\mu$m long rectangular-shaped ring lasers will reach their COIL respectively. For the 94 $\mu$m long rectangular-shaped ring laser, its COIL can be as low as 89.3%. Such a power reflectivity is viable by combining dry etching and golden deposition processes.

In addition, Fig. 6 also shows that the shorter the cavity length, the more sensitive both the internal loss of rectangular-shaped ring laser and the modulation bandwidth of EOIL laser to the power reflectivity of TRMs. Therefore, the higher power reflectivity and the more rigorous control of reflectivity are required for the rectangular-shaped ring laser with a shorter cavity length. Moreover, as the power reflectivity of the TRMs is irrelevant to the cavity length, the higher modulation bandwidth can be expected when a shorter rectangular-shaped ring laser as a slave laser. Taking the power reflectivity of the TRMs is 96% as an example, the internal loss corresponding to the cavity lengths of 63 $\mu$m, 94 $\mu$m and 126 $\mu$m are 19.2 cm$^{-1}$, 14.8 cm$^{-1}$ and 12.7 cm$^{-1}$, respectively. The modulation bandwidth of EOIL lasers corresponding to different ring cavity lengths is about 38 GHz, 35 GHz and 30 GHz, respectively (see Fig. 5). Even though the reflectivity of the TRMs is reduced to 90.4%, the modulation bandwidth of 27.2 GHz is still achievable. Therefore, it is truly feasible to employ a rectangular-shaped ring laser as the slave laser in a monolithically integrated EOIL system indeed.

## IV. CONCLUSION

In this paper, we systematically investigated the modulation response of monolithically integrated EOIL semiconductor ring lasers based on photon-photon resonance effect theoretically. Our analysis indicated that the modulation response of EOIL lasers strongly depends on the internal loss of the ring lasers. The modulation bandwidth of as high as 67.5 GHz was predicted on the assumption that the waveguide was loss-free. However, in the real world, when the loss associated with the bending loss in the case of circular-shaped waveguide, or the loss related to the reflectivity of the TRMs in the case of rectangular-shaped waveguide configuration, was accounted, the picture was very different. In fact, it was found that EOIL with circular-shaped ring laser is no longer a choice for applications which require the modulation bandwidth performance over 25 GHz, due to the excessive loss associated with the bending waveguide. Nonetheless, the high bending loss could be circumvented by employing rectangular-shaped ring laser, since the loss is only dependent reflectivity of the TRMs, in this scenario. Our simulation indicated that it is possible to achieve the modulation bandwidth better

than 38 GHz, provided the reflectivity of the TRM is greater than 96%. Therefore, it shows in principle that a monolithically integrated EOIL laser with high modulation bandwidth can be realized indeed by using a rectangular-shaped ring laser.

## REFERENCES

[1] H. Liu, C. F. Lam, and C. Johnson, "Scaling optical interconnects in datacenter networks opportunities and challenges for WDM," in *Proc. 18th IEEE Symp. High Perform. Interconnects*, 2010, pp. 113–116.

[2] F. Kish *et al.*, "From visible light-emitting diodes to large-scale III–V photonic integrated circuits," *Proc. IEEE*, vol. 101, no. 10, pp. 2255–2270, Oct. 2013.

[3] A. Abbasi *et al.*, "43 Gb/s NRZ-OOK direct modulation of a heterogeneously integrated Inp/Si DFB laser," *J. Lightw. Technol.*, vol. 35, no. 6, pp. 1235–1240, Mar. 2017.

[4] A. Abbasi *et al.*, "43 Gb/s NRZ-OOK direct modulation of a heterogeneously integrated Inp/Si DFB laser," *J. Lightw. Technol.*, vol. 35, no. 6, pp. 1235–1240, Mar. 2017.

[5] T. Shindo *et al.*, "GaInAsP/InP lateral-current-injection distributed feedback laser with a-Si surface grating," *Opt. Exp.*, vol. 19, no. 3, pp. 1884–1891, Jan. 2011.

[6] A. E. Siegman, *Lasers*. Mill Valley, CA, USA: Univ. Science Books, 1986.

[7] S. Yamaoka *et al.*, "Directly modulated membrane lasers with 108 GHz bandwidth on a high-thermal-conductivity silicon carbide substrate," *Nature Photon.*, vol. 15, pp. 28–35, 2021.

[8] H. Sung, E. K. Lau, and M. C. Wu, "Optical properties and modulation characteristics of ultra-strong injection-locked distributed feedback lasers," *IEEE J. Sel. Topics Quantum Electron.*, vol. 13, no. 5, pp. 1215–1221, Sep./Oct. 2007.

[9] Z. Liu and R. Slavík, "Optical injection locking: From principle to applications," *J. Lightw. Technol.*, vol. 38, no. 1, pp. 43–59, Jan. 2020.

[10] E. J. Bochove, "Theory of modulation of an injection-locked semiconductor diode laser with applications to laser characterization and communications," *J. Opt. Soc. Amer. B-Opt. Phys.*, vol. 14, no. 9, pp. 2381–2391, Sep. 1997.

[11] M. I. Memon, B. Li, G. Mezosi, Z. Wang, M. Sorel, and S. Yu, "Modulation bandwidth enhancement in optical injection-locked semiconductor ring laser," *IEEE Photon. Technol. Lett.*, vol. 21, no. 24, pp. 1792–1794, Dec. 2009.

[12] L. Chrostowski and W. Shi, "Monolithic injection-locked high-speed semiconductor ring lasers," *J. Lightw. Technol.*, vol. 26, no. 19, pp. 3355–3362, Oct. 2008.

[13] G. A. Smolyakov and M. Osinski, "High-speed modulation analysis of strongly injection-locked semiconductor ring lasers," *IEEE J. Quantum Electron.*, vol. 47, no. 11, pp. 1463–1471, Nov. 2011.

[14] G. A. Smolyakov, Y. Fichou, and M. Osinski, "Analysis of high-frequency modulation response of strongly injection-locked cascaded semiconductor ring lasers," *IEEE J. Quantum Electron.*, vol. 48, no. 12, pp. 1568–1577, Dec. 2012.

[15] J. Troger, P.-A. Nicati, L. Thevenaz, and P. A. Robert, "Novel measurement scheme for injection-locking experiments," *IEEE J. Quantum Electron.*, vol. 35, no. 1, pp. 32–38, Jan. 1999.

[16] H. Kawaguchi, *Bistabilities and Nonlinearities in Laser Diodes*. Boston, MA, USA: Artech House, 1994.

[17] C. Born, M. Sorel, and S. Yu, "Linear and nonlinear mode interactions in a semiconductor ring laser," *IEEE J. Quantum Electron.*, vol. 41, no. 3, pp. 261–271, Mar. 2005.

[18] E. K. Lau, H. K. Sung, and M. C. Wu, "Scaling of resonance frequency for strong injection-locked lasers," *Opt. Lett.*, vol. 32, no. 23, pp. 3373–3375, Dec. 2007.

[19] R. Lang, "Injection locking properties of a semiconductor laser," *IEEE J. Quantum Electron.*, vol. QE-18, no. 6, pp. 976–983, Jun. 1982.

[20] E. K. Lau, H.-K. Sung, and M. C. Wu, "Frequency response enhancement of optical injection-locked lasers," *IEEE J. Quantum Electron.*, vol. 44, no. 1, pp. 90–99, Jan. 2008.

[21] E. K. Lau, L. J. Wong, X. Zhao, Y. Chen, C. J. Chang-Hasnain, and M. C. Wu, "Bandwidth enhancement by master modulation of optical injection-locked lasers," *J. Lightw. Technol.*, vol. 26, no. 15, pp. 2584–2593, Aug. 2008.

[22] X. Wang and L. Chrostowski, "High-speed Q-modulation of injection-locked semiconductor lasers," *IEEE Photon. J.*, vol. 3, no. 5, pp. 936–945, Oct. 2011.